Dose distributions of MV photon beams in heterogeneous media

Author: Mireia Martos Marsiñach
Advisor: Dr. José M. Fernández Varea
*Facultat de Física, Universitat de Barcelona, Martí i Franquès 1, 08028 Barcelona, Catalonia**

Abstract: In this project we studied the dose distributions of 6 and 15 MV photon beams in a heterogeneous phantom which contains layers of lung-equivalent material. We compared measurements done at the Hospital de la Santa Creu i Sant Pau with the results of Monte Carlo simulations using the PENELOPE/penEasy program and the predictions of the AAA and Acuros algorithms. We also studied the quality index of our beams and the relation between dose to water and dose to medium.

I. INTRODUCTION

One of the most common oncological treatments is radiotherapy with MV photon beams. Many aspects have to be considered before a patient undergoes radiotherapy. One of them is to know with an accuracy better than 2% the distribution of absorbed dose in the irradiated tissues.

This project consists in the comparison between experimental data taken at the Hospital de la Santa Creu i Sant Pau (HSCSP), simulation results and the predictions of two algorithms. We wanted to investigate the dose distribution of photon beams of 6 MV and 15 MV in a phantom with a lung heterogeneity. The simulations were done using the PENELOPE/penEasy Monte Carlo code. The studied algorithms were AAA and the newer Acuros [1,2]. Our hypothesis was that Acuros is better than AAA to model the dose distribution in heterogeneities.

There is an ongoing debate about whether it is better to report absorbed dose to medium (D_m), considering the actual medium where the dose is deposited, or dose to water (D_w), recalling that the radiation damage is mostly inflicted to the cell nuclei, which are essentially of liquid water. In this context we have studied the relation between $D_{m,}$ and D_w, which involves the stopping-power ratio $s_{w,m.}$[3].

An important aspect in this type of studies is the *quality* of the beam, which refers to its penetration capability and is related to the nominal energy. It is not possible to make all the beams equal because every machine and manufacturers are different and their generated photon energy spectra too. To specify beam quality the $TPR_{20,10}$ index is recommended in the TRS-398 protocol [4]. We have checked the $TPR_{20,10}$ of the 6 and 15 MV beams delivered by the linac at the HSCSP. We used the aforementioned algorithms to calculate D_m and D_w as a function of depth and compare them with the simulated data. All the analysis and conclusions obtained are presented in sections III and IV below.

II. MATERIALS AND METHODS

A. Experimental data

As we mentioned above, we obtained our experimental data at the HSCSP using a Varian CLINAC 2100 C/D linear accelerator. This machine has a gantry that delivers x-ray beams of 6 and 15 MV. The photons pass through the primary collimator and a flattering filter. Then, jaws delimit the shape that we want to irradiate on the phantoms, which were laying on the treatment table. One phantom consisted of five 5-cm-thick slabs, alternating plastic water and lung, see Fig 1 (left). The mass densities of plastic water and lung were 1.03 g/cm^3 and 0.2955 g/cm^3, respectively. We wanted to study D_m and D_w so we also used another phantom made of plastic water. The source-to-surface distance was fixed to 100 cm and the selected field size was 10 × 10 cm^2.

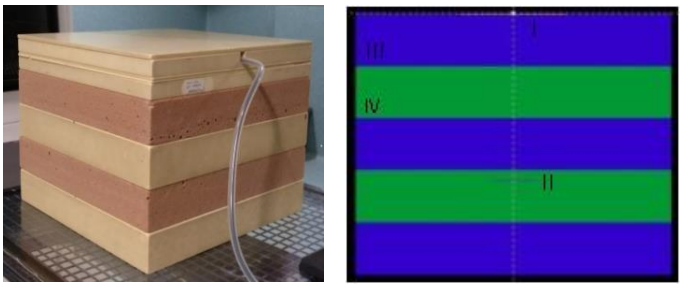

FIG. 1: Phantom with two lung inserts used at the HSCSP for the measurement of D_w (left) and the geometry reproduced with PENELOPE (right).

We employed a NACP02 plane-parallel ionization chamber coupled to an electrometer and our measurements were made at 24.3 ºC and 760.1 mmHg. We placed the detector along the *z* axis at depths ranging from 0.5 cm to 23 cm. We also made a Computed Tomography (CT) study to the phantom to then obtain our D_m and D_w data.

* Electronic address: mireia.martos@hotmail.com

B. Algorithms

To obtain the D_m and D_w data we used the software Eclipse, which incorporates the algorithms AAA and Acuros. AAA (Analytical Anisotropic Algorithm) is an algorithm for the calculation of dose distributions for photon beams, superposing the dose deposited by two photon sources (primary and secondary) and an electron contamination source. On the other hand, Acuros is a grid-based Boltzmann equation solver, which performs accurate and rapid radiotherapy dose calculations [1]. AAA only reports D_w whereas Acuros can provide D_w and D_m [2]. Both algorithms give a continuous dose distribution function as a function of depth once the parameters of the experiment are fixed.

C. Monte Carlo simulations

For the simulations we used the software PENELOPE (PENetration and Energy LOss of Positrons and Electrons). Monte Carlo simulation consists in the generation of random showers of primary particles (photons, in our case) in the material(s) of the geometry of interest. The program follows the trajectories of the primary particles as well as the secondary particles produced in the various interactions within the material.

In our study we used the main program penEasy [5]. To run a simulation with PENELOPE/penEasy we need, at least, three files: the geometry of the experiment, the corresponding material(s) and the input file.

C.I. Geometry definition

The aim of any simulation is to try to reproduce the experiment as faithfully as possible. In PENELOPE, the geometry is described with bodies delimited by quadric surfaces or other bodies. The general equation for a "canonical" quadric is [5]

$$F(r) = I_1x^2 + I_2y^2 + I_3z^2 + I_4z + I_5 \qquad (1)$$

The indices I_i take the values -1, 0 or 1. Then, if needed, one applies scaling, rotation and translation. In this way, we can create any quadric that we want. For instance, if we define $I_1 = 1$, $I_2 = I_3 = I_4 = 0$ and $I_5 = -1$

$$F(r) = x^2 - 1 \qquad (2)$$

which gives the pair of planes $x = \pm 1$.

To define the complete geometry we have to declare all the surfaces that delimit the various bodies. We can also have a body inside another one. In such cases we need to set the elements from inside out. That is, first we should define the innermost one. The aim was trying to reproduce the geometry of the phantom we used at the HSCSP, Fig. 1 (left). The simulated geometry is shown in Fig.1 (right).

To reproduce the experiment with penEasy we have simulated a phantom of 30x30x30 cm3 and then we have divided the volume in five alternating layers of plastic water (blue) and lung (green). We have also included a field of 10x10 cm^2 at the surface of the phantom and a detector which moves along the *z* axis in every simulation to study the dose as a function of depth.

The number 1 in Fig. 1 (right) represents the detector, number 2 the field and numbers 3 and 4 the plastic water and lung slabs, respectively. To create this geometry we have declared 16 surfaces and 7 bodies.

C. II. Material files

To achieve a realistic simulation we also have to use cross sections for the materials of the irradiated phantom. Plastic water is among the materials in the PENELOPE database. But the composition of the Saint Bartholomew's lung used in the experiment and the inflated ICRU lung included in PENELOPE's database differ too much. Hence, we had to create a material file entering the exact composition and mass density of the experimental one.

C.III. Input files

The input file is the one that sets the characteristics of the simulation and links the geometry, material and energy spectrum files. For the latter we adopted the spectra of 6 MV and 15 MV from Varian [6]. We have simulated 10^8 particles to achieve statistical uncertainties well below 1%. Electrons and positrons are absorbed when their kinetic energy falls below 200 keV. In turn, photon simulation is discontinued at 10 keV.

As we wanted to study the change of the dose with the depth, we selected twenty points belong the *z* axis: 1, 2, 3, 5.5, 6, 7, 8, 10.5, 11, 12, 13, 15.5, 16, 17, 18, 20.5, 21, 22 and 23 cm. (20 points in total). We created a specific geometry for each case (just moving the scoring region to the appropriate place). Taking into account that we had two beams and we wanted both D_m and D_w, this implies a total of 80 simulations. In addition, we needed four simulations to evaluate the $TPR_{20,10}$ and three more to calculate the $s_{w,m,}$ factor that relates D_m with $D_{w.}$ We will explain these seven simulations with more detail below.

D. Determination of beam quality

To have an quantitative measure of the penetration of our beams we use the $TPR_{20,10}$ index [4], defined as the ratio of absorbed doses at depths of 20 cm and 10 cm,

$$\mathrm{TPR}_{20,10} = \frac{D_{20\,\mathrm{cm}}}{D_{10\,\mathrm{cm}}} \qquad (3)$$

The motivation for this index is that it is not affected by the low-energy (and therefore less penetrating) electron contamination of the x-ray beam. To calculate $TPR_{20,10}$ for the 6 MV and 15 MV beams, we run four simulations (two for each beam) using the geometry displayed in fig. 2.

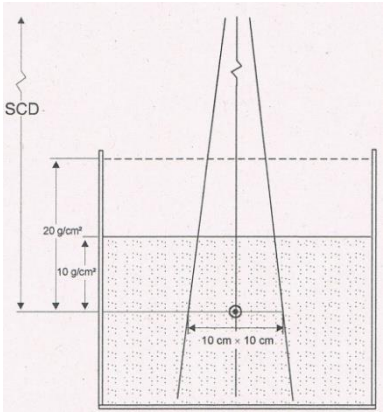

FIG 2: Geometry used to calculate $TPR_{20,10}$ for photon beams. SCD refers to the source-to-chamber distance, which is kept constant at 100 cm. The chamber is placed at depths of 10 cm and 20 cm. The field size is 10 × 10 cm^2 at the position of the chamber. Figure taken from reference [4].

E. Relation between D_m and D_w

In this project we have also studied the relation between D_m and D_w. This relation is given by the relation [3]

$$D_w = D_m \, s_{w,m} \qquad (4)$$

introduced by Gray in his cavity theory. The water-to-medium stopping-power ratio $s_{w,m}$ is [3]

$$s_{w,m} = \frac{\int_0^{E\max} (\emptyset_E)_m \, (S_{el}/\rho)_w \, dE}{\int_0^{E\max} (\emptyset_E)_m \, (S_{el}/\rho)_m \, dE} \qquad (5)$$

where $(\emptyset_E)_m$ is the differential energy fluence (electrons per unit energy and surface), obtained from Monte Carlo simulation, and S_{el}/ρ is the mass electronic stopping power of each medium. The Appendix summarizes the Bethe-Bloch formula required to evaluate the electronic stopping power [3]. We prepared a Fortran program to compute $s_{w,m}$ from Eq. (5).

We run three simulations to determine $(\emptyset_E)_m$ for the 6, 15 and 18 MV beams. The latter was used to compare the corresponding $s_{w,m}$ with the value quoted in reference [7].

III. RESULTS

First of all, we will discuss the qualities of our beams, comparing those measured at the HSCSP with the ones resulting from our Monte Carlo simulations. Table I shows the results obtained.

TABLE I: $TPR_{20,10}$ values for the 6 MV and 15 MV beams measured at the HSCSP and simulated with PENELOPE/penEasy.

Type	Beam	$TPR_{20,10}$
HSCSP	6 MV	0.6657
Monte Carlo	6 MV	0.661(6)
HSCP	15 MV	0.7607
Monte Carlo	15 MV	0.755(5)

We can see from the table that the $TPR_{20,10}$ of the simulated beams do not differ much from the experimental ones, which supports the reliability of our simulations. To achieve better agreement between experiment and simulation we would need the photon energy spectra actually delivered by the linac at the HSCSP, e.g. obtained from a full simulation of the gantry. However, this is well beyond the scope of the present project.

Next we are going to analyze our percentage depth-dose distributions (PDD, i.e. normalized to 100%) and the predictions of the two algorithms. Fig. 3 displays D_w for the 6 MV case.

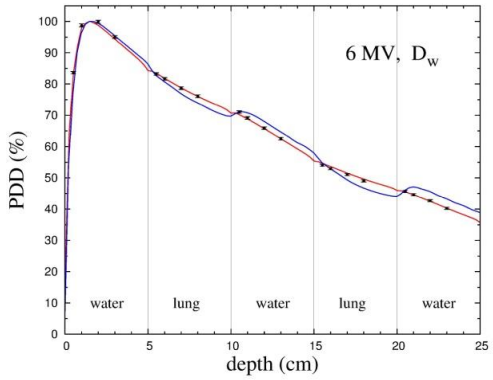

FIG 3: PDDs D_w for the 6 MV photon beam. The black circles are our Monte Carlo values. The blue and red curves are the results of AAA and Acuros, respectively.

We can see that Monte Carlo and Acuros match really well. This does not happen for AAA because this algorithm is less accurate to account for the presence of heterogeneities. AAA works well in the first water slab but then moves away from the Monte Carlo and Acuros values.

To further assess the reliability of our data, we have calculated the ratios

$$\frac{D(z)^{*}_{w\ or\ m}/D(zref)^{*}_{w\ or\ m}}{D(z)^{exp}_{w}/D(zref)^{exp}_{w}} \quad (6)$$

* means that we have calculated the same ratio for the Monte Carlo, AAA and Acuros absorbed doses. "w or m" indicates that we have also evaluated both the D_w and D_m data. We have made four plots, shown in Fig. 4.

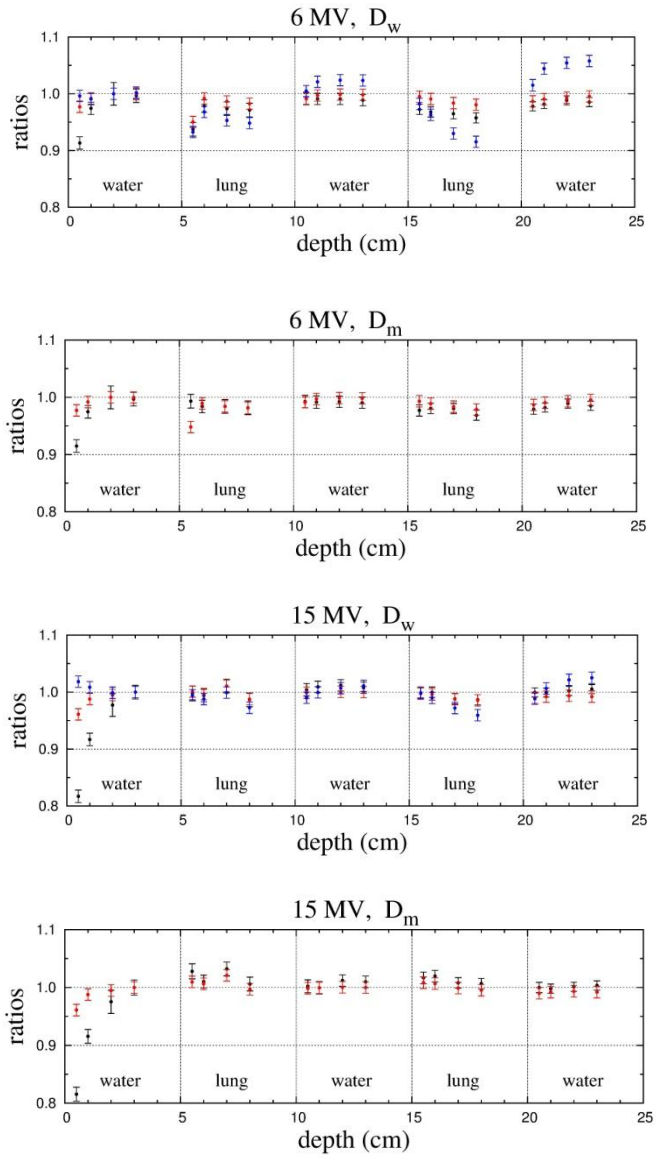

FIG 4: Ratios of absorbed for 6 MV and 15 MV photon beams. The Monte Carlo values are plotted in black, Acuros in red and AAA in blue.

We observe that in general we have achieved good statistics in our results. The Monte Carlo and Acuros data are close to 1, i.e. they are close to the measured values. However, AAA results differ a little bit more from the experiment, as we can appreciate.

Showing our results in this way lets us compare the studied algorithms but it is not the best way to see the differences between D_m and D_w. This is why we have prepared Tables II and III below, where we display our calculated $s_{w,m}$ values.

TABLE II: $s_{w,m}$ values for SB lung.

SB lung	6 MV	15 MV
$s_{w,m}$	1.006	1.000

TABLE III: $s_{w,m}$ values for ICRU lung.

ICRU lung	6 MV	18 MV
$s_{w,m}$	0.997	0.986

The $s_{w,m}$ factors published in ref. [7] for ICRU lung are 0.998 for 6 MV and 0.987 for 18 MV, almost identical to our results (Table III). This gives us confidence in the accuracy of the values in Table II for SB lung, which will be used in the subsequent analysis.

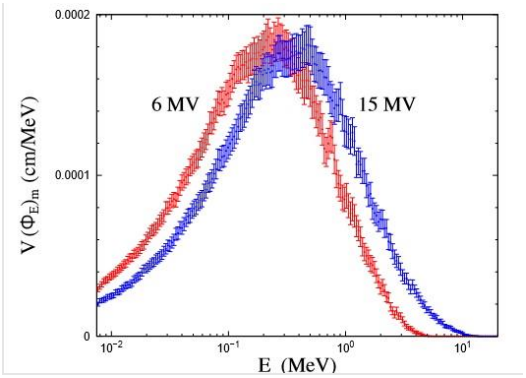

FIG 5: Simulated energy fluences for 6 and 15 MV photon beams.

In this figure we can see the $\emptyset_E$ distributions used to calculate the $s_{w,m}$ factors. Notice that as less energetic is a beam, as more to the left has it's highest energetic peak.

TABLE IV: D_w and D_m results from Monte Carlo simulations (6 MV) for the points inside SB lung. The last column tabulates the product D_m $s_{w,m}$.

	6 MV		
z (cm)	D_w (fGy/hist)	D_m (fGy/hist)	D_m $s_{w,m}$ (fGy/hist)
5.5	0.539(5)	0.527(4)	0.531(9)
6	0.528(5)	0.516(4)	0.521(9)
7	0.509(5)	0.500(4)	0.502(9)
8	0.492(5)	0.483(4)	0.485(8)
15.5	0.350(3)	0.341(3)	0.345(7)
16	0.342(3)	0.337(3)	0.337(6)
17	0.330(3)	0.326(3)	0.326(6)
18	0.317(3)	0.312(3)	0.313(6)

TABLE V: D_w and D_m results from Monte Carlo simulations (15 MV) for the points inside SB lung. The last column tabulates the product $D_m\, s_{w,m}$.

	15 MV		
z (cm)	D_w (fGy/hist)	D_m (fGy/hist)	$D_m\, s_{w,m}$ (fGy/h)
5.5	0.981(4)	0.981(5)	0.966(9)
6	0.965(4)	0.952(5)	0.950(9)
7	0.933(4)	0.925(5)	0.918(9)
8	0.904(4)	0.896(5)	0.890(8)
15.5	0.698(3)	0.690(4)	0.687(8)
16	0.688(3)	0.681(4)	0.691(7)
17	0.661(3)	0.655(4)	0.650(7)
18	0.641(3)	0.635(4)	0.631(7)

In Tables IV and V we can appreciate that the differences between D_m and D_w are small for both 6 MV and 15 MV beams. Studying those points inside lung tissue, we have compared the D_w data obtained by Monte Carlo simulations and by using the $s_{w,m}$ factor to convert D_m into D_w. We can see that both results agree very well, showing the usefulness of the Bragg-Gray cavity theory.

IV. CONCLUSIONS

We have calculated the $TPR_{20,10}$ of our 6 MV and 15 MV beams by Monte Carlo simulations and find that they match with the experimental values of the linac at the HSCSP. Hence, the x-ray spectra adopted in our simulations are similar to those actually delivered by the linac.

In second place, we have compared the absorbed doses obtained by Monte Carlo simulations and the AAA and Acuros algorithms to experimental data. We find that the PENELOPE/penEasy program provides accurate results and that the Acuros algorithm fits better than AAA to the measurements, as we had hypothesized in the introduction. We conclude that this new algorithm is better than the older AAA, and helps to improve the reliability of treatment planning at the hospital.

Finally, we have evaluated the small differences between D_m and D_w data for lung and assessed the validity of Bragg-Gray's cavity theory.

Acknowledgments

First of all I would like to thank my advisor Dr. J.M. Fernández-Varea for guiding me during all the realization of this project. I also want to thank Dr. Pablo Carrasco, radiophysicist at the HSCSP for helping with the experiment and teaching me the basics of dosimetry. Finally, I am grateful to my parents and friends for their support.

Appendix

We present there the specific equations used to calculate the mass electronic stopping power [3]

$$S_{\text{el}} = NZ\frac{2\pi e^4}{m_e c^2 \beta^2}\left\{ln\left(\frac{E^2}{I^2}\frac{\gamma+1}{2}\right) + f^{(\pm)}(\gamma) - \delta\right\} \quad (7)$$

where N is the number of atoms per unit volume, Z is the atomic number, E is the electron's kinetic energy and I is the mean excitation energy; m_e is the electron mass, c is the speed of light and e is the elementary charge. Besides,

$$\beta = \frac{v}{c} \quad (8)$$

the Lorentz factor is

$$\gamma = \frac{1}{\sqrt{1-\beta^2}} \quad (9)$$

and

$$f^{-}(\gamma) = \gamma^{-2}\left[1 - (2\gamma-1)\ln 2 + \frac{1}{8}(\gamma-1)^2\right] \quad (10)$$

Finally, we adopted a simple parameterization of the density-effect correction

$$\delta = a[X_1 - \log_{10}(\beta\gamma)]^m + 2\ln\left(\frac{\gamma E_p}{I}\right) - 1 \quad (11)$$

Here E_p is the nominal plasma energy of the medium whereas a, X_1 and m are fitting parameters.

[1] O.N. Vassiliev *et al*, *Phys. Med. Biol.* **55**, 581 (2010).

[2] A. Van Esch *et al*, *Med. Phys.* **33,** 4130 (2006).

[3] *Fundamentos de Física Médica. Volumen 1: Medida de la Radiación*, edited by A. Brosed (ADI, Madrid, 2011) chapters 1 and 4.

[4] IAEA, *Determinación de la dosis absorbida en radioterapia con haces externo*, TPR 398 (OIEA, Viena, 2005) chapter 6.

[5] F. Salvat, *PENELOPE-2014. A Code System for Monte Carlo Simulation of Electron and Photon Transport'* (OECD/NEA, Issy-les_Moulineaux, 2015) chapters 1 and 7.

[6] D. Sheikh-Bagheri and D.W.O. Rogers, *Med. Phys.* **29**, 391 (2002).

[7] J.M. Fernández-Varea, P. Carrasco, V. Panettieri and L. Brualla, *Phys. Med. Biol.* **52**, 6475 (2007).

[8] *Handbook of Radiotherapy Physics.* Edited by P. Mayles, A. Nahum and I.C. Rosenwald. (Taylor and Francis Group, 2007).